3-2021

Adaptive simultaneous pervasive visible light communication and sensing

Ila Nitin GOKARN
Singapore Management University, ingokarn.2019@phdcs.smu.edu.sg

Archan MISRA
Singapore Management University, archanm@smu.edu.sg

Citation

GOKARN, Ila Nitin and MISRA, Archan. Adaptive simultaneous pervasive visible light communication and sensing. (2021). *2021 IEEE International Conference on Pervasive Computing and Communications Workshops and other affiliated events (PerCom Workshops): March 22-26, Kassel, Germany: Proceedings*. 344-347.

Available at: https://ink.library.smu.edu.sg/sis_research/6945

PerCom Work in Progress on Pervasive Computing and Communications 2021
DOI: 10.1109/PerComWorkshops51409.2021.9431014

Adaptive & Simultaneous Pervasive Visible Light Communication and Sensing

Ila Gokarn, Archan Misra
Singapore Management University
{*ingokarn.2019, archanm*}*@smu.edu.sg*

***Abstract*—Driven by the rapid growth in the proliferation of low-cost LED luminaries, *visible light* is being increasingly explored as both a high-speed communication and sensing channel for a variety of IoT applications. Visible Light Communication (VLC) exploits the high-frequency modulation of an optical source while ensuring imperceptibility to the human eye. In parallel, recent approaches in Visible Light Sensing (VLS) have demonstrated how high frequency optical strobing can be used to perform vision-based remote sensing of mechanical vibrations (e.g., of factory equipment). To date, exemplars of VLC and VLS have, however, been explored in isolation, without consideration of their mutual dependencies. In this work, we explore future visible light-based pervasive computing scenarios, where strobing and high-frequency signal modulation are used concurrently to support both VLC and VLS. We demonstrate that there is in fact a fundamental tradeoff between the desires for high VLC throughput and wide VLS coverage: such a tradeoff is driven by the duty cycle of the strobing light source, such that a larger duty cycle results in higher communication throughput but reduced sensing resolution, and vice versa. We then discuss two approaches under exploration to overcome this limitation (i) Alternating VLC and VLS mechanisms in a single-LED system (ii) Multi-harmonic adaptive strobing in a multi-LED system.**

***Index Terms*—VLC, Visible Light Sensing, Adaptive System, Edge Computation**

I. Introduction

Visible Light Communications (VLC) has been touted as an extremely promising mechanism for unobtrusive, high bit rate, device-to-device communication [1] in a variety of pervasive environments, including factory floors [2], and warehouses. VLC's rise has been facilitated by the rapid growth in the use of LED lighting, whose very low O(μsec) switching transient enables modulation of the visible light channel at frequencies high enough to be imperceptible to human occupants. More recently, visible light has also been used as a *sensing* mechanism, in tandem with commodity cameras or photodiodes, to capture both relatively low-frequency human motion & gestures [3] and high-frequency machine vibration [2]. In such Visible Light Sensing (VLS) paradigms, LED lights are effectively strobed at a variety of frequencies, helping to shift the *observed* vibration frequencies to a lower range, where they can be recovered via commodity (typically 30-120 FPS) camera sensors.

While each of these phenomena has been individually studied, there has been almost no investigation of the possibility of *simultaneously* supporting VLC and VLS. This is an important gap, as a unified framework for high-frequency strobing and modulation of visible light signals can enable a more comprehensive class of pervasive industrial and IoT-based applications. For example, as shown in Figure 1, a mobile robot equipped with an LED array could be used to both communicate control commands via VLC to industry equipment equipped with a simple photodiode-based receiver and simultaneously sense machine vibration frequencies. Conceptually, such simultaneous VLC and VLS enables visible light to mimic the recent trend of using wireless (especially WiFi) as a means for not just data communication, but also passive sensing [4] and even energy harvesting [5].

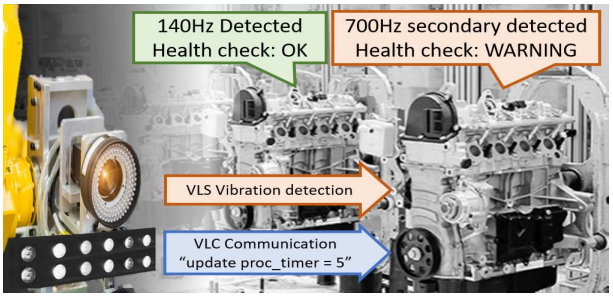

Fig. 1. Factory Floor Robot performing simultaneous VLC and VLS of Machine Vibrations

In this paper, we address this lacunae by presenting the first-ever mathematically rigorous approach for understanding how characteristics of the visible light source affect the interplay between VLC goodput (application-level communication throughput) and VLS coverage/accuracy. Using basic principles of frequency domain analysis, we first show that these two metrics exhibit a *natural tradeoff*, driven primarily by the *duty cycle* (d) of the strobing light source. Intuitively, VLS ideally assumes the use of a strobing source with infinitesimally small duty cycle (so-called Dirac-Delta pulses [6]). However, the VLC goodput is directly proportional to the active period of each individual pulse and thus benefits from a progressive increase in the duty cycle (which, however, effectively destroys the strobing phenomena needed for VLS).

Subsequently, we shall utilise this understanding of the underlying dynamics of VLS and VLS to discuss mechanisms that improve the achievable VLS-VLS tradeoff. Overall, we believe that our work will contribute to a foundational understanding of the interplay between VLC and VLS performance, and will eventually contribute to the design of future pervasive systems that utilize visible light for both communication and sensing.

II. Background & Mathematical Fundamentals

A. Stroboscopic Principle and Camera Based Sensing

We first mathematically model a classical VLS system, where a single stroboscopic light source is used to illuminate an object vibrating with an unknown frequency, with the resulting image captured through a low frame-rate camera. Assuming the vibration source has a vibrating signal $\omega_v(t)$ consisting of a single (sinusoidal) frequency component ω_v (for ease of explanation), and is sampled by an infinite strobing pulse train *(Dirac comb)* $p(t)$ such that $p(t) = \sum_{n=-\infty}^{\infty} \delta(t - nT_s)$ with a known time period T_s (i.e., with a strobing frequency $\omega_s = \frac{1}{T_s}$), the resulting sampled signal $x_s(t)$ can be represented as:

$$x_s(t) = \omega_v(t) \times p(t) \tag{1}$$

The Fourier domain representation of Equation 1 is:

$$\begin{aligned} X_s(\omega) &= \frac{1}{2\pi}[X(\omega_v) \otimes P(\omega_s)] \\ &= \frac{1}{2\pi}[\delta(\omega_v) \otimes \frac{2\pi}{T_s} \sum_{k=-\infty}^{\infty} \delta(\omega - k\omega_s)] \\ &= \frac{1}{T_s} \sum_{k=-\infty}^{\infty} \delta(\omega_v - k\omega_s) \end{aligned} \tag{2}$$

where $\otimes$ denotes convolution in the frequency domain. In effect, the resulting signal consists of an infinite set of sinusoids, obtained by shifting the object's vibration frequency ω_v via an integral value of ω_s. The resulting sampled signal $X_s(\omega)$ is then observed through a low frame-rate camera (e.g. $\omega_{cam} = 30$ fps), which essentially acts as a low pass filter that eliminates frequencies outside the range $\lfloor \frac{-\omega_{cam}}{2}, \frac{\omega_{cam}}{2} \rfloor$. An image processing pipeline, which measures the displacement of the object observed across such consecutive camera frames, is then used to compute the *observed* vibration frequency ω_p.

To ensure that a single vibration frequency generates only a single frequency peak ω_p within the camera's observational range, the proposed approach in [6] sets the camera frequency (frame rate) to be *identical* to the fundamental strobe frequency—i.e., $\omega_{cam} = \omega_s$. Accordingly, the possible values of the *unknown* vibration frequency will satisfy the equation $\omega_v = \omega_p \pm k\omega_s \quad \forall k \in \mathbb{Z}$. However, estimation of the unknown vibration frequency ω_v by a single strobe frequency is then ambiguous, as a peak in the camera-observed motion frequency can correspond to any arbitrary integer-valued choice of k. To tackle this problem, VLS approaches such as [6] utilize a set of consecutive strobes, each performed at a distinct *mutually prime* frequency, with the camera frame rate adjusted to match the current strobe frequency. This yields two different choices of observed strobing and estimated peaks $(\omega_{s1}, \omega_{p1})$ and $(\omega_{s2}, \omega_{p2})$ which satisfy the following relationship:

$$\omega_v = \omega_{p1} + k\omega_{s1} = \omega_{p2} + l\omega_{s2} \text{ for } k, l \in \mathbb{Z} \tag{3}$$

By applying the Chinese Remainder Theorem and exploiting the fact that ω_{s1} and ω_{s2} are mutually prime, one can rapidly determine the unique values of (k,l) that satisfy the above equation and thereby recover the unknown vibration frequency ω_v.

B. Binary Frequency Shift Keying on Strobing Light

Conventional VLC does not utilize a strobing signal, but instead utilizes an appropriate modulation scheme (e.g., Binary Frequency Shift Keying or BFSK) to execute high-frequency adjustment of the intensity of the LED light source. When adapted to a combined VLS+VLC scenario, such modulation is applied to the non-zero portion (the ON period) of the strobe signal. It is important to observe that any real-word strobe has a finite ON period (in contrast to the VLS analysis performed above, which assumed each pulse width to be infinitesimal). We assert that the BFSK-based modulation of the LED intensity does not impact the VLS capability (this has also been empirically confirmed in [7]) as the camera-based processing pipeline is based purely on the ability to observe the vibrating object whenever the LED is ON, and does not depend on the actual intensity of the LED source (assuming that the trough of the high-frequency BFSK modulated ON signal is strong enough to permit tracking of the vibrating object).

III. Theoretical Model of VLS-VLC Trade-off

Currently VLS techniques utilize a strobing light source, where the light behaves as an impulse train, with T_a less than 1% of T_s, i.e., the duty cycle $d = \frac{T_a}{T_s}$ is less than 1% [6], [7]. Clearly, as VLC is possible only during the ON period of the light source, a low duty cycle is prejudicial to high data rates: $d = 1\%$ implies an effective loss of 99% of the maximum transmission capacity.

The solution then is to increase the duty cycle, effectively morphing the strobe signal from an impulse train to a *rectangular* pulse train (whose pulse width is determined by the duty cycle). However, we shall now mathematically and quantitatively demonstrate that this transition, to higher duty cycle values, is prejudicial to VLS operation, as it effectively reduces the range of vibration frequencies that are suitably shifted within the camera's range of observation frequencies $\lfloor \frac{-\omega_{cam}}{2}, \frac{\omega_{cam}}{2} \rfloor$.

In general, an arbitrary rectangular strobe signal is represented as a sum of constituent sinusoids by the Fourier synthesis equation:

$$p(t) = a_0 + \sum_{n=1}^{\infty} a_n \cos(2\pi\omega_s tn) - \sum_{n=1}^{\infty} b_n \sin(2\pi\omega_s tn) \tag{4}$$

where $n \in Z^+$, ω_s is the frequency of the strobe, and the coefficients "a" and "b" denote the real and imaginary magnitudes in the frequency spectrum. For rectangular pulse trains with duty cycle=d, Equation 4 yields the following Fourier Series analysis equations:

$$a_0 = X_a d, \qquad a_n = \frac{2X_a}{n\pi} \sin(n\pi d), \quad b_n = 0 \tag{5}$$

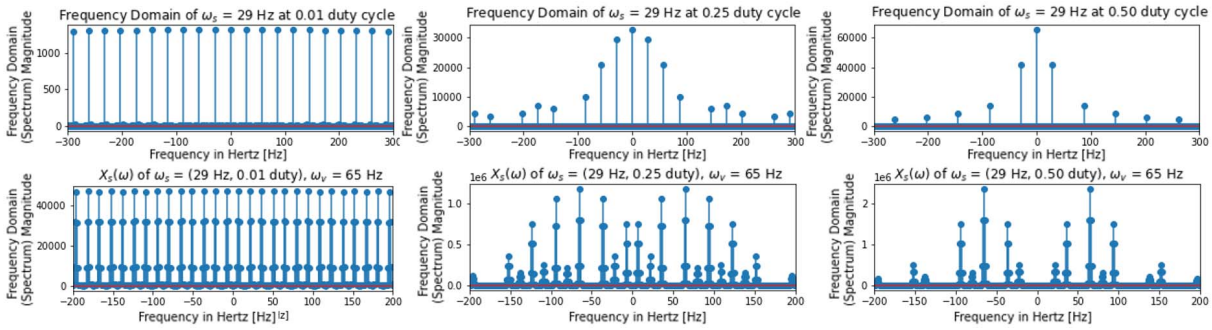

Fig. 2. Amplitude of strobe harmonics, and resulting vibration frequency shifts, for different Duty Cycles (d). $a_n = 0$ for every $(100/d)^{th}$ harmonic.

Here a_0 represents the strobe signal's DC component, while a_n denotes the amplitude of the the n^{th} harmonic of the fundamental strobe frequency ω_s.

Analysis of Equation 5 leads to the following observations:

1) Depending on the duty cycle, some of the harmonics of ω_s will yield $a_n = 0$. If $a_n = 0$, this implies that the corresponding frequency shifted component $\omega_v - n * \omega_s$ is absent in the Fourier domain representation of $X_s(\omega)$ (Equation 2).
2) If impulse signals are modeled as $d = 1\%$ rectangular pulse waves, the 100^{th} harmonic would have a_{100} = 0. If the 100^{th} harmonic of ω_s is larger than ω_{max} (the maximum range of vibration frequencies being monitored), it follows that any unknown vibration frequency ω_v in the range $(0, \omega_{max})$ will manifest as a shifted peak in the camera's range $\lfloor \frac{-\omega_{cam}}{2}, \frac{\omega_{cam}}{2} \rfloor$. This is the *implicit* assumption used in current VLS systems.
3) As the duty cycle increases, more harmonics of ω_s (more specifically, every $(100/d)^{th}$ harmonic) have their amplitudes of $a_n = 0$. In addition, with increasing d, the amplitude of higher-order non-zero harmonics, relative to the D.C. component (0 Hz), also diminishes (as $\frac{a_0}{a_n} \propto \frac{d}{sin(d)}$ is an increasing function of d). Consequently, an even larger number of harmonics have insufficient intensity (below a minimum threshold Min_{th}) to manifest as ω_p or 'peaks' in the observed camera signal.

The above analysis leads to the conclusion that higher duty cycles, while resulting in higher VLC throughput, result in an increased fraction of ω_s to have $a_n = 0$ (missing harmonics) or have $a_n < Min_{th}$ (weak and unobservable harmonics). Figure 2 illustrates this phenomenon quantitatively, for $d = \{1\%, 25\%, 50\%\}$. The graphs on top plot the frequency response of just the strobe signal $P(\omega_s)$, whereas the graphs at the bottom plot the resulting frequency-shifted harmonics of the observed signal $X_s(\omega)$ for ω_v =65Hz & ω_s =29Hz. We see, for example, that for $d = 25\%$, every 4^{th} harmonic of ω_s, denoted by a_{4i}, $= 0$. As a consequence, vibration frequencies that lie in the range (considering only the positive frequencies) $(\lfloor 0, \frac{\omega_{cam}}{2} \rfloor + 4 * i * \omega_s, i \in \mathbb{Z}^{0+}$ will be unobservable, due to the absence of the corresponding harmonic component needed to 'shift' ω_v to the observation range $\lfloor \frac{-\omega_{cam}}{2}, \frac{\omega_{cam}}{2} \rfloor$. This phenomenon is most exacerbated for d =50% where every even harmonic is missing.

Key Finding: The above analysis demonstrates how and why the *duty cycle* effectively controls the tradeoff between VLC and VLS efficiency. A larger duty cycle leads to a greater ON period and thus a higher VLC bit rate, but also leads to the loss of a greater number of harmonics of ω_s, thereby creating 'blind spots' in the observable vibration frequency range.

A. Quantifying Duty Cycle vs. VLS/VLC Tradeoff

We now quantitatively derive the sensing coverage ratio by considering a single strobe system at ω_s 29Hz at varying duty cycles (d ={1%, 10%, 25%, 50%}), thereby enabling *simultaneous operation* of VLC and VLS. We limit d to 50% as higher values causes the rectangular pulse signal to lose its stroboscopic nature, due to the dominant DC signal. We assume ω_{max} = 1000Hz i.e. the system attempts to infer vibration frequencies only within the (0,1000) Hz range. For each value of d, we calculate the specific set of missing and weak harmonics (harmonics whose intensity is less than an empirically set $Min_{th} = 1\%$ of the DC component a_0), and thereby determine the collection of *unobservable* vibration frequencies that lie in the interval $\omega \in [a_n - \omega_s/2, a_n + \omega_s/2]$ of each such harmonic a_n.

We also calculate the expected VLC goodput (assuming no bit decoding loss) for each of these duty cycles. Note that the absolute VLC goodput is dependent on the specific values of ω_s (number of strobes/sec) and b (number of bits per strobe), which are hardware/technology dependent. As our analysis is based on mathematical fundamentals and is technology-agnostic, we express goodput as a percentage of the maximum ideal goodput.

Figure 3 plots this resulting tradeoff between VLC goodput and VLS coverage (fraction of frequency range that is observable) as a function of d. At d =1%, 96.6% of frequencies can be detected but achieves ∼0% goodput. As the duty cycle increases, the VLC goodput increases linearly, while the VLS coverage drops due to the missing harmonics in $P(\omega_s)$. At d =50%, we are able to achieve 81.4% goodput, but at the cost of ∼51% reduction in the VLS coverage.

IV. Discussion

Moderating this VLS-VLC tradeoff is key to enabling a new class of pervasive applications. Two mechanisms that show

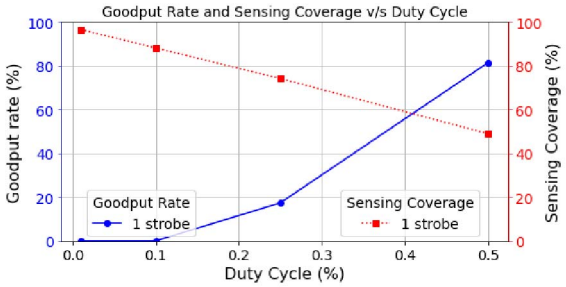

Fig. 3. Tradeoff between VLC goodput and VLS coverage vs. duty cycle for a single strobe

promise rely on the design of LED lights in the system.

The first mechanism is a single-LED system, where VLS pulses with duty cycle $d = 1\%$ are triggered during the OFF period (or $T_s - T_a$) of the primary VLC signal of any duty cycle $1\% < d < 99\%$, thereby achieving *alternating or parallel* VLC and VLS operation. Relying on system-level intelligence, the VLC receiver photodiode discards signals received during the OFF period of the VLC signal and the VLS observer camera retains only those frames that pertain to VLS operation in order to ascertain the unknown vibration ω_v. Note that this approach embeds the strobe signal within the single LED being used for VLC, and may thus not be amenable to multi-LED strobing systems, such as the multi-harmonic approach to be discussed next.

The second mechanism is based on a multi-LED system, which introduces the concept of *harmonic multi-strobing*, where the primary strobe is accompanied by an additional set of LED lights which strobe at integral multiples of the base strobe frequency. These additional lights do not participate in VLC, but help to create a *virtual* set of strobes with lower duty cycle, which effectively improves the achievable VLS-VLC tradeoff by recovering some of the "missing" harmonics. Nonetheless, the harmonic multi-strobing approach, which utilizes a single fixed duty cycle, is unable to fully and accurately infer all possible vibrating frequencies and suffers from sensing "blind spots". System-level intelligence or an *adaptive mechanism* can iteratively adjust the (duty cycle, number of harmonic strobes) combination until it is able to unambiguously sense and infer the unknown vibration frequency, while simultaneously maintaining reasonable goodput.

In our ongoing work, we are exploring both of these approaches, and shall embed them into a practical prototype system for joint VLC and VLS. Additional parameters like number and synchronicity of the LED lights in a multi-LED system, photodiode diversity and range of the overall signal, and chosen duty cycle parameters, all determine the formal theory, system implementation, and complexity of simultaneous and adaptive VLS-VLC systems.

V. Related Work

In the field of VLS, a variety of authors [2], [7] have demonstrated the principles of how LED strobing can enable such vibration sensing using cheap, low frame-rate commodity cameras. On the other hand, modern VLC technologies (e.g.,IEEE 802.15.7) provide high-speed, wireless communication throughput of nearly 100 Mbps, with research prototypes achieving ∼1Gbps [1]. Relatively little work has explored the joint execution of VLC and VLS. Varshney et. al. propose a VLS system [3] that performs gesture recognition via sensing of light variations on solar cells, while using RF backscatter to communicate sensor readings using O($10\mu W$) power. More recently, Amjad & Dressler have explored using the same strobing light source to achieve both communication and sensing of mechanical vibrations [7]–while they do not explore the tradeoffs presented here, they demonstrate that the low frame-rate camera's operation is unaffected by the high-frequency VLC signal.

VI. Conclusion

We have discussed the ability to perform VLS and VLC simultaneously, a capability important for many novel IoT-based industrial and consumer applications. We first established the conflicting choices imposed by VLS and VLC on a strobe's duty cycle: while VLC favors a higher duty cycle, VLS requires as low a duty cycle as possible to ensure that high frequency vibration signal are shifted within the observational range of a low-FPS commodity camera. We then briefly outline two alternative approaches that can alleviate this tradeoff: (a) careful interleaving of VLS strobe during the OFF period of a VLC-modulated signal, and (b) multi-LED harmonic strobing. System-level intelligence with adaptive mechanisms are key in both approaches to achieve both high VLC goodput and VLS coverage. Future work should explore the formal system definition of these approaches and possible extension of this to a more distributed environment, where a distributed set of LED lights are used to support *multiple concurrent* streams of VLC communication and spatially dispersed VLS-based sensing.

References

[1] A. H. Azhar, T.-A. Tran, and D. O'Brien, "A gigabit/s indoor wireless transmission using mimo-ofdm visible-light communications," *IEEE photonics technology letters*, vol. 25, no. 2, pp. 171–174, 2012.

[2] D. Roy, A. Sinharay, B. Bhowmick, R. Rakshit, T. Chakravarty, and A. Pal, "A novel rf-assisted-strobe system for unobtrusive vibration detection of machine parts," *IEEE Sensors Journal*, 2020.

[3] A. Varshney, A. Soleiman, L. Mottola, and T. Voigt, "Battery-free visible light sensing," in *Proceedings of the 4th ACM Workshop on Visible Light Communication Systems*, 2017, pp. 3–8.

[4] R. Ravichandran, E. Saba, K.-Y. Chen, M. Goel, S. Gupta, and S. N. Patel, "Wibreathe: Estimating respiration rate using wireless signals in natural settings in the home," in *Pervasive Computing and Communications (PerCom), 2015 IEEE International Conference on*. IEEE, 2015, pp. 131–139.

[5] V. H. Tran, A. Misra, J. Xiong, and R. K. Balan, "Wiwear: Wearable sensing via directional wifi energy harvesting," in *2019 IEEE International Conference on Pervasive Computing and Communications, PerCom, Kyoto, Japan, March 11-15, 2019*. IEEE, 2019, pp. 1–10.

[6] D. Roy, A. Ghose, T. Chakravarty, S. Mukherjee, A. Pal, and A. Misra, "Analysing multi-point multi-frequency machine vibrations using optical sampling," in *Proceedings of the 1st International Workshop on Internet of People, Assistive Robots and ThingS*, 2018, pp. 55–59.

[7] M. S. Amjad and F. Dressler, "Integrated communications and non-invasive vibrations sensing using strobing light," in *ICC 2020-2020 IEEE International Conference on Communications (ICC)*. IEEE, 2020, pp. 1–6.